

BSSD 2021 Performance Metric Q4

Goal: Develop new omics-based techniques to understand microbiome function in environmental samples

Q4 Target: Report on the use of imaging and mass spectrometry-based capabilities to describe microbiome interactions.

Introduction

The LLNL “Microbes Persist” Soil Microbiome Scientific Focus Area (SFA) seeks to determine how microbial soil ecophysiology, population dynamics, and microbe-mineral-organic matter interactions regulate the persistence of microbial residues and formation of soil carbon (C). In much of our research, we use imaging, mass spectrometry, and related methods to study plant-microbe-mineral interactions, viral and microbial particles from soil, and the signatures plant and microbial necromass contribute as part of soil organic matter (SOM). Our project’s signature techniques include NanoSIMS-enabled approaches (to understand cell-cell and OM-mineral interactions at the single cell and even viral particle scale), radiocarbon (^{14}C) analyses (to determine both the age and turnover time of soil organic matter), and a suite of soil chemical characterization techniques we describe below, and collectively refer to as ‘*Multi-dimensional SOM-mineral characterization*’ (SEM, TEM, STXM, NEXAFS, NMR, FTICR-MS, LC-MS). In this report, we focus on how imaging, NMR, beamline and mass spectrometry approaches can deepen our understanding of soil microbiomes and their engagement with the soil matrix.

Mass Spectrometry Imaging: NanoSIMS-based approaches

With LLNL’s high-resolution imaging mass spectrometer (CAMECA NanoSIMS 50)—one of only ~50 instruments in the world—we perform stable isotope probing (tracing rare isotopes of C, O, N and other elements) and high spatial resolution isotopic mapping of cell-cell, viral and OM-mineral interactions, using a technique called ‘*NanoSIP*’¹⁻⁷. This method allows the activity of individual microbial cells to be probed within a complex sample. Typically, substrates are labeled with ^{13}C and/or ^{15}N , though other isotopes, including radioactive isotopes, can be used. This method is particularly valuable when combined with other imaging methods, such as fluorescence microscopy and X-ray microscopy, which provide complementary information. In recent work, we investigated the transport of ^{15}N via ammonium gas by arbuscular mycorrhizal fungi (AMF) (Fig. 1). NanoSIP allowed us to analyze the fungi in association with roots and show that the fungi were likely engaged in N transport because they were highly enriched in ^{15}N ⁸.

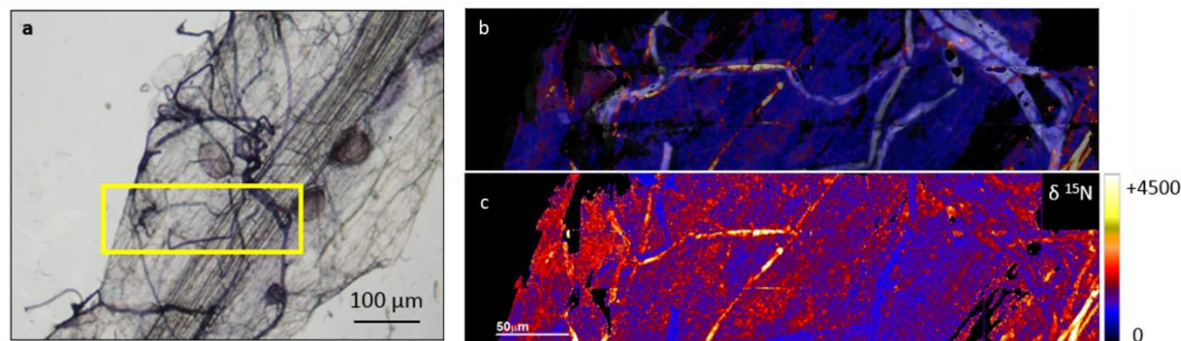


Figure 1. Light microscopy (a) and NanoSIMS images (b & c) of a mycorrhizae-colonized root following exposure to $^{15}\text{NH}_3$. (a) Fungal hyphae and vesicles growing inside and around the root are stained in dark blue. The yellow box indicates the region analyzed by NanoSIMS in (b) & (c). (b) Sulfur ion image shows hyphae that are on the root surface. (c) The $\delta^{15}\text{N}$ NanoSIMS image shows ^{15}N enrichment.

NanoSIP can also be used to track the accumulation of microbial or plant residues on mineral surfaces. In another recent study, we imaged fungal transport of ^{13}C derived from decaying fungal mycelia necromass to goethite mineral surfaces (**Fig. 2**; ⁹). NanoSIP distinguished fungal hyphae on the mineral surface from adsorbed dissolved organic matter and show that fungal hyphae represent a significantly larger transport mechanism than aqueous transport.

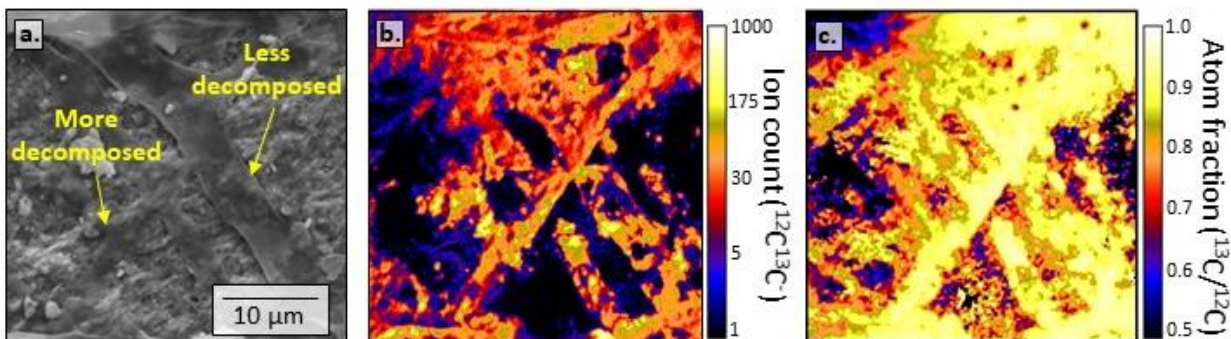


Figure 2. Panel (a) shows a scanning electron microscope (SEM) image of fungal hyphae in various stages of decay along the surface of a goethite particle. Panel (b) shows a correlated NanoSIMS ion image, revealing that the spatial distribution of organic molecules across the microsite (as $^{12}\text{C}^{13}\text{C}$ ion counts after ~ 100 nm of sputtering) was concentrated along the hyphal tracks. Panel (c) is a NanoSIMS atom fraction image revealing high ^{13}C enrichment (78-95 atom percent) across the surface, demonstrating that the majority of C transferred to the goethite during the incubation originated from the decomposing fungal substrate (located ≤ 1 mm away). Collectively, these images suggest that most of the fungal necromass C accumulation on minerals during this experiment was transferred via saprotrophic hyphal exploration, rather than by diffusion through soil water.

In a third soil fungal transport study, we used NanoSIP imaging to visualize the transformation and association of root-derived C with surfaces of different mineral types. In this study, we grew *Avena barbata*, a Mediterranean annual grass, in soil microcosms within a 99 atom% $^{13}\text{CO}_2$ atmosphere and traced ^{13}C fixed by the plant as it moved from roots into soil fungi and then onto fresh mineral surfaces ¹⁰. In the rhizosphere, the high ^{13}C enrichment we see in fungal hyphae (**Fig. 3**) indicates they must have been arbuscular mycorrhizal fungi (i.e., biotrophs that acquire their cellular C from the host plant). These fungi appear to play an important role in shuttling C from roots to minerals ¹¹, a conclusion further supported by our LC-MS lipidomics results (see below).

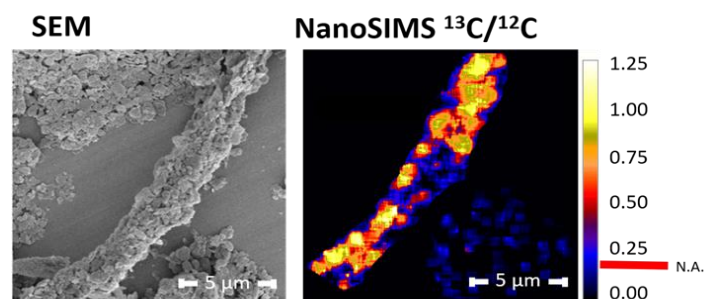


Figure 3. Images of fungal hyphae and kaolinite incubated in the rhizosphere of *A. barbata* (wild oat grass) grown in a $^{13}\text{CO}_2$ enriched atmosphere. (a) scanning electron micrograph (SEM) and (b) complementary NanoSIMS images of ^{13}C enrichment.

NanoSIP phage and viral imaging

Viral ecology is a rapidly developing field, that has only recently been embraced in soil science ¹². We hypothesize that viruses play a significant role in soil C cycling and are developing methods and the tools to characterize their functions. NanoSIP has the potential to provide data on the distribution of activity of soil viruses, including rates of microbial lysis and virus production, the percentage of active viruses, the quantity of microbial C liberated, and the fate of microbial and viral C post-lysis. In previous work, we and others have shown that nanoSIP has sufficient

sensitivity to quantify the isotopic enrichment of larger viruses (>100 nm diameter)^{13,14}. However, previous work also indicated that analysis of bacterial viruses (phage) would be challenging due to their small size (~ 50 nm diameter). Recently, we demonstrated the ability to extract viral particles from isotope tracer experiments in the lab and field and detect ¹³C and ¹⁸O enrichment in those samples. We have also collected preliminary data that suggests that new NanoSIMS instrument capabilities can characterize the activity of bacteriophage down to 50 nm based on isotopic enrichment (**Fig. 4**). We are currently optimizing sample preparation and electron microscopy imaging methods for soil phage and viruses.

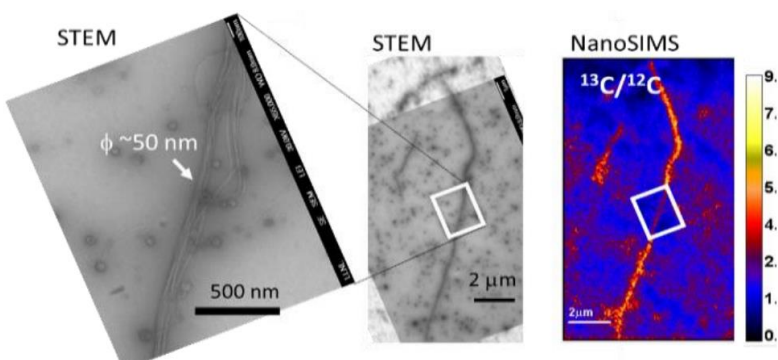


Figure 4. Correlated scanning transmission electron microscopy (STEM) and NanoSIMS images of ¹³C enriched M13 virions in a bundle ~50 nm in diameter. Note that the area image at high resolution was altered but still detected.

ChipSIP: NanoSIMS and phylogenetic microarrays to link microbial identity and function

The ‘*Chip-SIP*’ method, developed at LLNL, uses NanoSIMS imaging to determine the isotopic enrichment of rRNA molecules hybridized to a phylogenetic microarray^{15,16} and can be used to identify the active microorganisms in complex environmental communities. Relative to the widely-used density-gradient SIP¹⁷ approach, the ChipSIP method has several benefits: it requires relatively low RNA enrichment (e.g., 0.5 atom% ¹³C), permits shorter isotope incubations, can assess multiple isotopic tracers in the same sample, targets RNA, and requires no amplification step. We have used this technique in many environments, including water, soil and insect gut¹⁸⁻²⁰. In a recent study, we used Chip-SIP to disentangle substrate preferences of microbes growing in an active rhizosphere where roots were decaying (detritosphere)²¹. We used two isotopic tracers (¹³C, ¹⁵N) to determine if soil microbes (bacteria, archaea, fungi, protists) preferentially consumed ¹³C-root exudates vs ¹⁵N-root litter. Most rhizosphere organisms incorporated resources from both fresh root exudates and detrital inputs, but had different preferences for detrital or root inputs (**Fig. 5**). Actinobacteria preferentially consumed root-litter within an active rhizosphere. Fungi tended to assimilate both ¹⁵N from litter and ¹³C-exudates equally, supporting previous results that saprotrophic fungi can channel fresh rhizodeposits into the soil food web²².

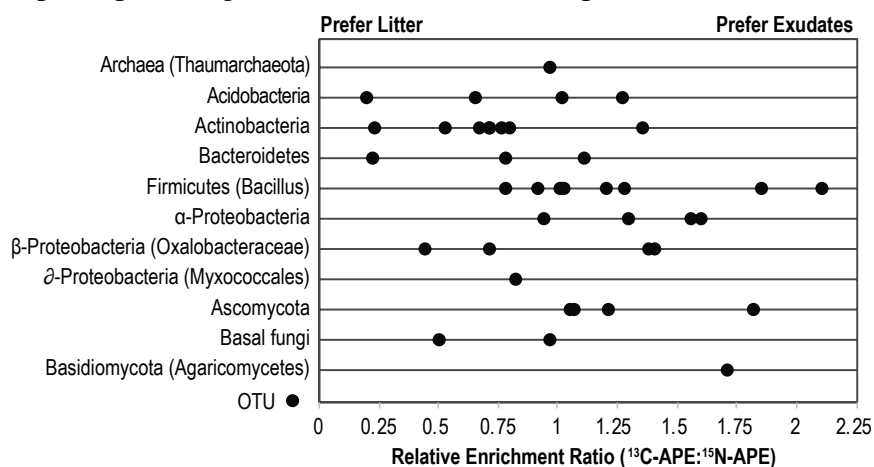


Figure 5. Relative substrate preferences for detrital ¹⁵N root litter versus ¹³C root exudates amongst bacterial, archaeal, and fungal populations detected by the Chip-SIP phylogenetic isotope array approach. Each dot represents an OTU (i.e., a distinct species within the soil microbiome). APE = atom percent excess

BulkSIP: Isotopic analysis of nanogram quantities of bulk DNA via NanoSIMS

NanoSIMS analysis can also quantify isotope enrichment in tiny amounts of total ('bulk') DNA or RNA extracted from a microbial community—this can provide important clues about average rates of substrate preference or consumption. Additionally, this approach can be used as a pre-screening step for density gradient SIP, to measure average isotope uptake (and thus confirm enrichment) prior to SIP processing. With our approach, which we call '*BulkSIP*', we analyze isotopic enrichment of bulk DNA and RNA for multiple elements (^{13}C , ^{15}N , ^{18}O) using NanoSIMS. Unlike other approaches that require microgram quantities of often precious DNA or RNA, our approach uses only ~100 ng while allowing us to analyze multiple isotopes simultaneously.

To show that NanoSIMS analysis of bulk DNA and RNA is quantitative, we produced nucleic acids standards with pure cultures of bacteria. BulkSIP analysis produced linear standard curves for a broad range of isotopic ^{13}C and ^{15}N DNA enrichments (**Fig. 6**). The slope of DNA standard curves decreased with sample concentration, indicating that the approach is sensitive to sample quantity. When we applied BulkSIP to a study of microbial activities in soil through time with three isotopically labeled substrates, we found that enrichment of ^{15}N and ^{18}O continued to increase throughout the duration of the incubation and enrichment values were highly correlated. This correlation supports the use of ^{18}O -BulkSIP as a metric for microbial growth.

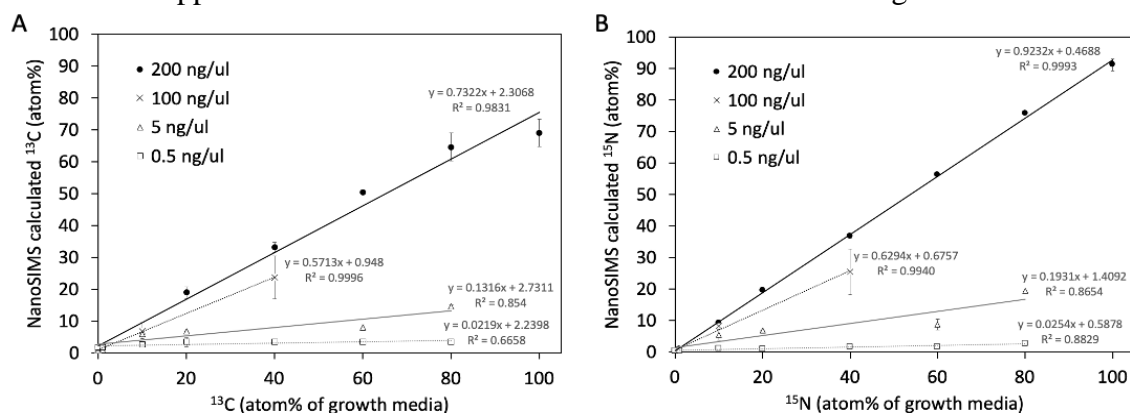


Figure 6. DNA standard curves created using *Pseudomonas stutzeri* DNA grown in defined media. Standard curves with different concentrations of DNA for A) ^{13}C and B) ^{15}N .

STXM-SIMS: Using isotope tracing and high-resolution spectro-microscopy to track formation of organo-mineral associations

While NanoSIMS and nanoSIP provide isotopic enrichment data at high spatial resolution, these methods yield only limited information about the molecular nature of a sample. Therefore, we have combined NanoSIMS with Scanning Transmission X-ray Microscopy (STXM) coupled with Near Edge X-ray Absorption Fine Structure spectroscopy (NEXAFS), a beamline approach that collects molecular information at a similar scale (~100 nm). Samples are analyzed first on the Lawrence Berkeley Lab Advanced Light Source (ALS) beamlines 5.3.2.2 and 11.0.2, to measure SOM classes (carbohydrate, lipid, protein, chitin) associated with minerals, and then later at LLNL on our NanoSIMS. The '*STXM-SIMS*' approach has the unique capacity to yield quantitative, *in situ* information on the molecular class and elemental quantity of isotope-enriched mineral-associated organic matter. We first demonstrated STXM-SIMS in 2012 to show that aliphatic C and amide N (microbial lipids and proteins) preferentially sorbed to Fe (hydr)oxides²³. Most recently, we used this approach on samples from a soil redox manipulation where ^{13}C plant litter had been added to a wet tropical soil. In this study, we partitioned the source of respired CO_2

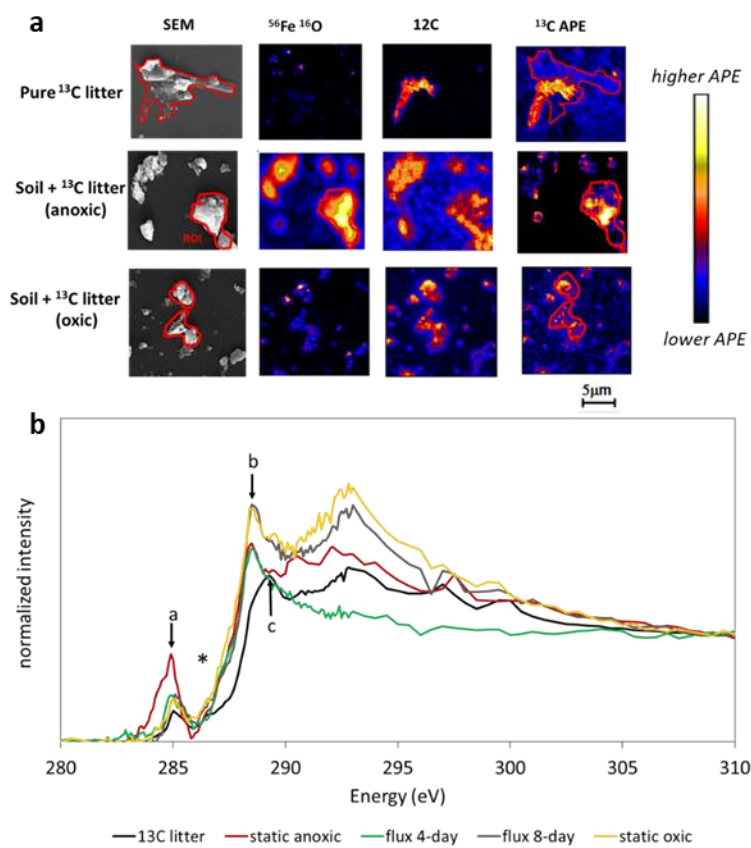


Figure 7: (a) Micrographs from a study where ^{13}C litter was added to a tropical soil and incubated under either anoxic or oxic conditions. SEM and corresponding NanoSIMS images of regions of interest where STXM/NEXAFS data had been collected. NanoSIMS images include: elemental (^{12}C) and ratio images (^{13}C atom percent excess (APE; $^{13}\text{C}^{12}\text{C}/^{12}\text{C}$) and Fe generated with $^{56}\text{Fe}^{16}\text{O}/^{12}\text{C}$ secondary ion counts). (b) NEXAFS data from the same regions of interest, including average carbon 1s for the pure ^{13}C litter and amended soils incubated under both static and oscillating redox regimes. Point marked with a, b and c indicate aromatic C, carboxyl/amide C and O-alkyl C peaks at 285, 288.6 and 289.5 eV (respectively). The asterisk indicates a C shoulder at ~ 287.5 eV, indicative of mineral-organic complexation.

powerful way to map both the molecular composition and isotopic enrichment of ^{13}C -labeled mineral-associated SOM.

Novel approaches for imaging soil and the rhizosphere:

Rhizo-scope: Multiphoton and coherent Raman imaging

Many of the research questions we are keen to explore in soil require the ability to document microbe-mineral, organic matter-mineral, microbe-root and food web interactions in an opaque matrix, ideally with high resolution, in real time and three dimensions. White light imaging in soil and the rhizosphere, however, is limited by poor contrast, scattering and absorption. Mass spectrometry-based imaging approaches are destructive and often require the sample to be fixed. Therefore, it is useful to have complimentary live imaging methods that allow researchers to

between native organic matter and amended-litter pools, and then used STXM /NEXAFS—NanoSIMS to measure how different soil redox regimes affected the chemical composition and spatial distribution of mineral-associated organic C. NanoSIMS results indicate that the ^{13}C -enriched material was highly dispersed within the mineral matrix and had become associated with Fe-oxides in both static and oscillating redox treatments (**Fig. 7A**). ^{13}C APE values indicated that the majority of the added ^{13}C litter had been microbially processed during the 44-day study, indicating microbes had equal access to the decaying litter irrespective of redox condition. However, STXM/ NEXAFS of the ^{13}C hotspots showed the decayed organic material differed in its C functional group composition. In static anoxic soils, aromatics accumulated on Fe-oxide surfaces, whereas in oxic soils O-alkyl residues were more common (**Fig. 7B**). These findings suggest that while oscillating redox regimes may not shift the bulk effect of decomposition on soil C pools, distinct soil redox regimes can cause differential SOC decomposition pathways. Our integrated STXM/SIMS approach, is a

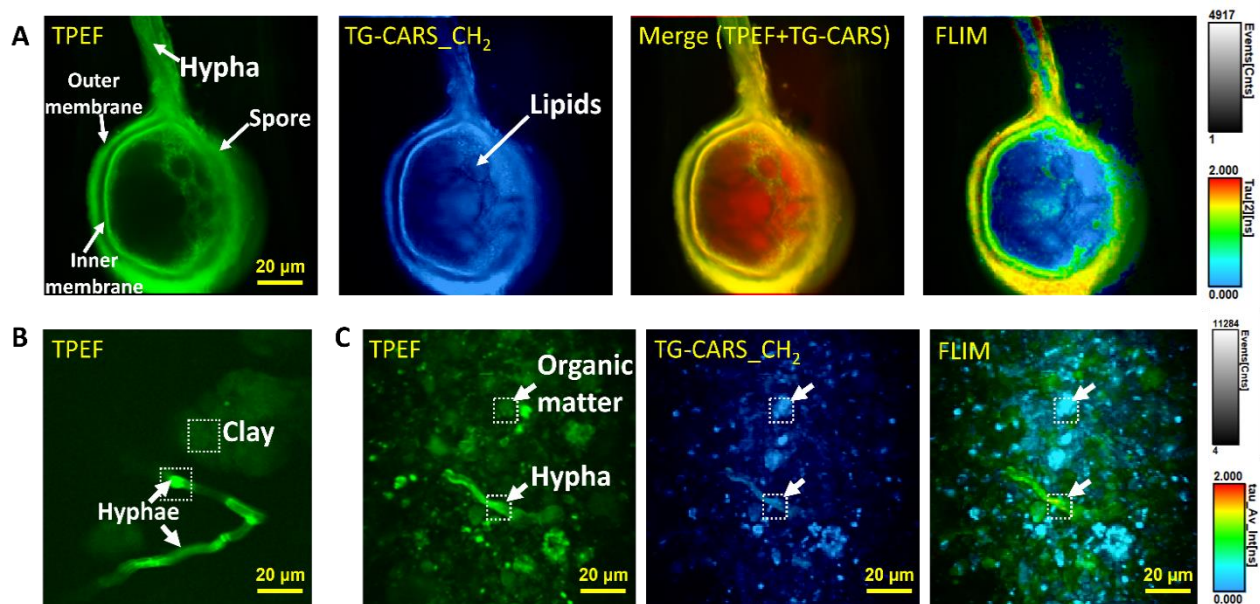


Figure 8. Label-free Rhizo-scope images of AMF *R. irregularis* spore and hyphae. (A) TPEF image shows hypha structure, and the TG-CARS signal shows the distribution of CH₂ moieties, including putative lipids inside the spore. The lipids and membrane structures are represented using different colormaps in the merged TPEF+TG-CARS and FLIM images. This image is an optical section of the spore. (B) Fungal structures generate strong TPEF (and CARS, not shown) relative to clay particles. (C) In natural soil, fungal structures can be identified based on the combination of morphology and chemistry (green in FLIM image). The FLIM grey scale indicates the number of photons detected per pixel, and the FLIM color scale indicates average photon arrival time in nanoseconds.

monitor development over time. To overcome these challenges, our LLNL team is developing the ‘*Rhizo-scope*’, which uses infrared light to generate multiple modes of contrast from soil and rhizosphere samples, including coherent anti-Stokes Raman scattering (CARS), two-photon excitation fluorescence (TPEF), second-harmonic generation (SHG), and sum-frequency mixing (SFM). With the Rhizo-scope, we have demonstrated imaging of live symbiotic fungi and bacteria within roots and minerals. TPEF gives broad imaging contrast; CARS provides chemical images of organic and inorganic compounds. Some minerals produce SHG and SFM photons. We also implemented fluorescence lifetime imaging (FLIM), which can deconvolve CARS from TPEF, and spectroscopy to characterize the detected signal in detail. We are working on implementing adaptive optics for the system, to enable deeper, higher sensitivity imaging in complex matrices. These capabilities will enable advanced live label-free imaging in the rhizosphere and soils. In recent studies using this instrument, we demonstrated 3D imaging of symbiotic arbuscular mycorrhizal fungi (AMF) in unstained plant roots (**Fig. 8**). TG-CARS allowed us to identify previously unknown lipid droplets in the symbiotic fungus, *Serendipita bescii*. We also visualized unstained putative bacteria associated with the roots of *Brachypodium distachyon* in a soil microcosm.

Mass spectrometry characterization of soil organic matter and metabolites

Fourier-Transform Ion Cyclotron Resonance Mass Spectrometry (FTICR-MS)

In many soil microbiome studies, it is critical to understand how cells are communicating with roots, each other, and contributing to SOM pools. Mass spectrometry-based capabilities including FTICR-MS and LC-MS can be used to fingerprint the *exometabolome*, the sum of small metabolites being produced or released into the soil matrix. In collaboration with colleagues at the

Environmental and Molecular Science Laboratory (EMSL), we have used these approaches to measure metabolite profiles and infer microbiome activities and interactions by comparing patterns from different soil treatments or C inputs. For FTICR-MS, we first extract microbe- and plant-derived compounds with a modified MPLE_x extraction protocol²⁴ and then characterize them using FTICR-MS (including a high field 21T instrument^{25, 26}). We typically identify broad patterns of chemical classes with Van Krevelen diagrams (e.g. lipids, proteins, carbohydrates, lignins, tannins) or plot them via multivariate approach such a Principal Components Analysis (PCA).

In the redox study described above (see *STXM-SIMS* section), we used FTICR-MS to screen for changes in organic compound classes following incubation under oxic, anoxic and oscillating regimes. Redox conditions significantly impacted soil microbiome decomposition activities in these tropical soils. Both anaerobic and aerobic heterotrophs were able to deplete labile, oxidized substrates released from fresh plant litter, however, reduced less thermodynamically favorable SOM was consumed differently by these two microbial consortia²⁷. In anoxic soils, we observed depletion of more oxidized water-extractable SOM (especially amino sugar-, carbohydrate-, and protein-like compounds), which likely served as substrates for anaerobic CO₂ production. Results from two-pool kinetic modeling showed that more frequent anoxic exposure limited decomposition of a slow-cycling C pool, but not a fast-cycling pool. These results suggest that aerobic and anaerobic heterotrophs were equally effective at degrading labile substrates that were released from fresh plant litter in this wet tropical soil, while aerobic decomposers were more effective in breaking down the potentially refractory compounds found in SOM.

In a more recent study, we have examined the effects of 12 weeks of drought on soil microbiomes and soil C stabilization. FTICR-MS data suggests the microbiomes associated with decaying roots produced significantly different metabolomes under drought conditions relative to control soils (**Fig. 9b**). This is in agreement with LC-MS measurements (Fig. 9a) (further discussed below). As drought conditions progressed, soil metabolites became gradually more reduced (**Fig. 9b**) as measured by the metabolite's average nominal oxidation state of carbon (NOSC)²⁸. In the droughted soils, the proportion of lignin-like compounds was elevated, while condensed hydrocarbons were suppressed relative to the control. Combining FTICR-MS formula assignments with LC-MS library identifications, we found that lignin-like compounds not only matched to oxidation products of lignin but also to secondary metabolites that have antioxidant, antimicrobial and antiviral properties. This suggests that multiple microbiome functions may lead to the greater percentage of lignin-like compounds under drought conditions.

To account for the fact that library databases include only a fraction of SOM components, we are also combining FTICR-MS derived molecular formula assignments with LC-MS based molecular networking to relate unknown molecular formulas to library matches. For example, lignin-like

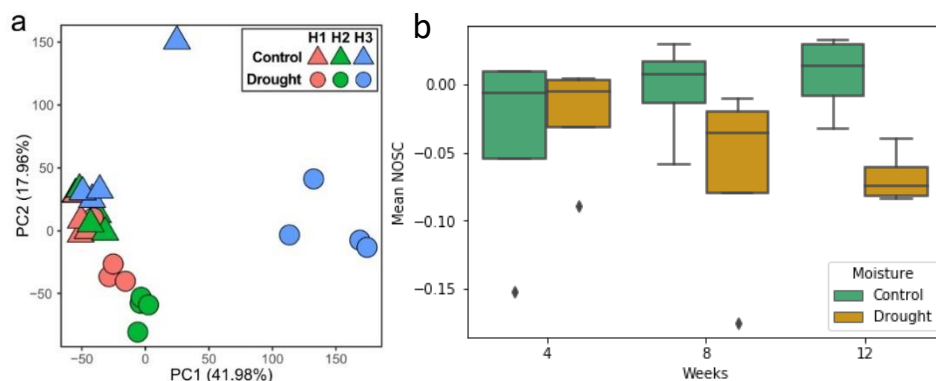


Figure 9. a) PCA of LC-MS metabolites from detritosphere samples taken at weeks 4, 8 and 12 (H1-3). b) Mean nominal oxidation state of C (NOSC) for FTICR-MS water soluble metabolites in drought (orange) or control (green) soil treatments.

molecular formulas detected using FTICR-MS have been matched to anthraquinone polyphenol metabolites detected using LC-MS. These putative identifications can be networked with other molecular formulas containing similar fragmentation spectra, which lack identifications (manuscript in prep). We believe this is a promising approach to corroborate molecular formula assignments, infer additional structural information for unknowns, and potentially allow for discovery of novel compounds in soils.

Lipidomics

Along with FTICR-MS, high resolution mass spectrometry (MS) coupled with liquid chromatography (LC) is one of the few approaches that has the chemical specificity necessary to determine the origins of organic matter. Specifically, lipids produced by different organisms, e.g. plants and microbes, can carry distinct signatures. In our study of how root-derived C becomes transformed and associated with surfaces of different mineral types (see Fig. 3 above), we used EMSL's LC-MS lipidomics approach to characterize OM on fresh minerals harvested after 2 months of incubation in greenhouse mesocosms¹⁰. Specifically, the samples were extracted with MeOH and analyzed for total lipids in both positive and negative modes, and lipids were fragmented using collision-induced dissociation. Confident lipid identifications were made using LIQUID (Lipid QUantitation and IDentification) as detailed in our recent paper¹⁰. Overall, we found more evidence of microbially-produced lipids than plant lipids on our mineral samples (Fig. 10). We think the hydrophobic nature of lipids may lead to mineral surface associations that are relatively persistent. As well, lipids seemed to associate strongly with kaolinite, which had the highest intensities for most lipid classes of all the mineral types we investigated. These results suggest that microbial processing is a key factor in organic matter associations with mineral surfaces.

Metabolomics

LC-MS metabolomics is being used even more often to characterize soil exometabolomes^{29, 30}, and has the added benefit of allowing for quantification and identification of metabolites using authentic standards. In the soil redox study described above, we used this approach in combination with ¹³C labeling to understand the impacts of redox conditions on microbial C cycling in soil. We found that oxic and fluctuating conditions resulted in similar metabolite profiles, while anoxic

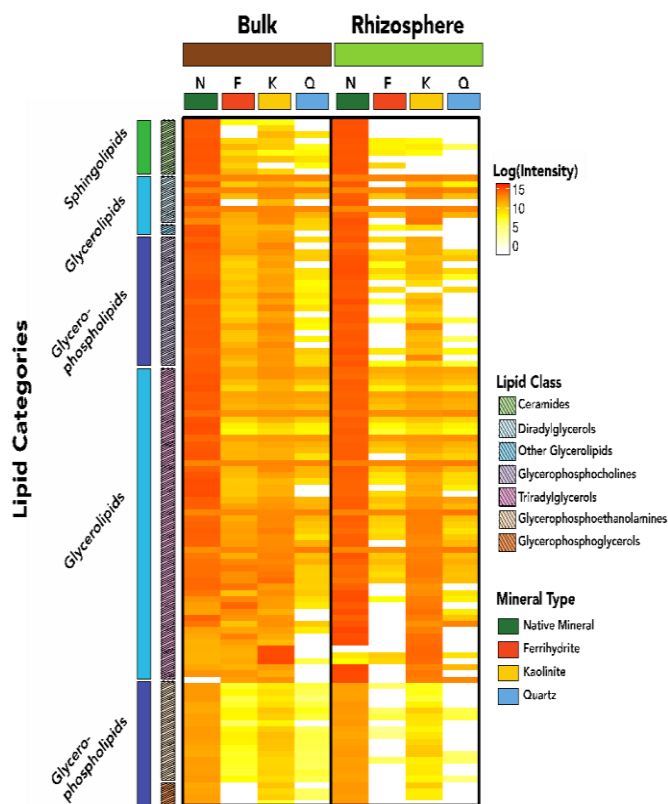


Figure 10. A heatmap of lipids identified in a LC-MS lipidomic analysis of minerals incubated in either rhizosphere or bulk soil for two months. Comparisons are made across treatment (bulk and rhizosphere) and mineral type (Native Mineral, Ferrhydrite, Kaolinite, and Quartz) (n=3). Due to differences in ionization potential, comparisons should only be made within lipid sub-class, rather than across broad lipid categories. Lipid intensities are log₁₀ transformed.

growth drove significant shifts in soil metabolome composition (**Fig. 11**). Of 206 metabolites identified, 41 were significantly enriched under anoxic conditions and 16 were significantly enriched under oxic/fluctuating conditions. By analyzing the isotopologues of individual metabolites, we are working to track C from ^{13}C labeled leaf litter and unlabeled soil C in the soil metabolome. We are also working to integrate this metabolite data with microbial community analyses from the same experiment to better understand the microbial contributions to C cycling under different redox conditions.

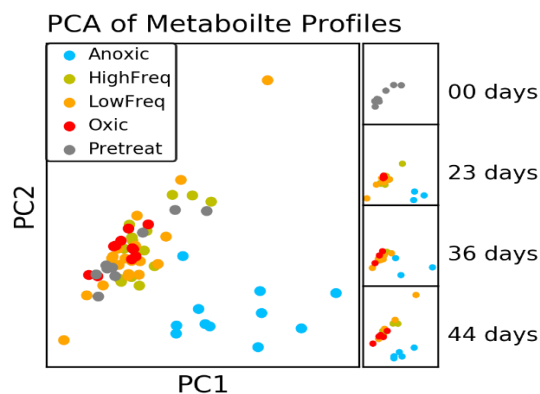


Figure 11. Principal component analysis of LCMS soil metabolite profiles from 0, 23, 36, and 44 days.

^{13}C -Nuclear Magnetic Resonance Spectroscopy (NMR)

NMR has been a standard technique for structural analysis of organic matter for years and is increasingly used for characterization of soil organic matter. Working with collaborators at EMSL, we used ^{13}C solid state NMR (500 MHz) to understand how organic matter associated with mineral surfaces changed through time and according to location in the soil ¹⁰. Major chemical classes of mineral-associated organic matter were identified by ^{13}C -NMR on samples collected after two months of incubation in lab mesocosm either in the presence or absence of roots. We focused on the 2-month timepoint because this is the period of peak plant growth and root exudation. Standards of potassium bromide, adamantane and a soil standard were also analyzed. The low C concentrations in our samples required long ^{13}C -NMR experiments, thus we ran pooled samples. We were unable to conduct analyses of Fe-oxide minerals due to their paramagnetism. This approach yielded two distinct insights that were not available through other approaches. First, we found that the overall organic chemistry of the mineral-associated organic matter was similar than what was found on native soil materials and a sample of kaolinite exposed to two months of rhizosphere dynamics (**Fig. 12**). Second, mineral associated C chemistry was very different outside of the rhizosphere and was dominated by saturated compounds, such as lipids.

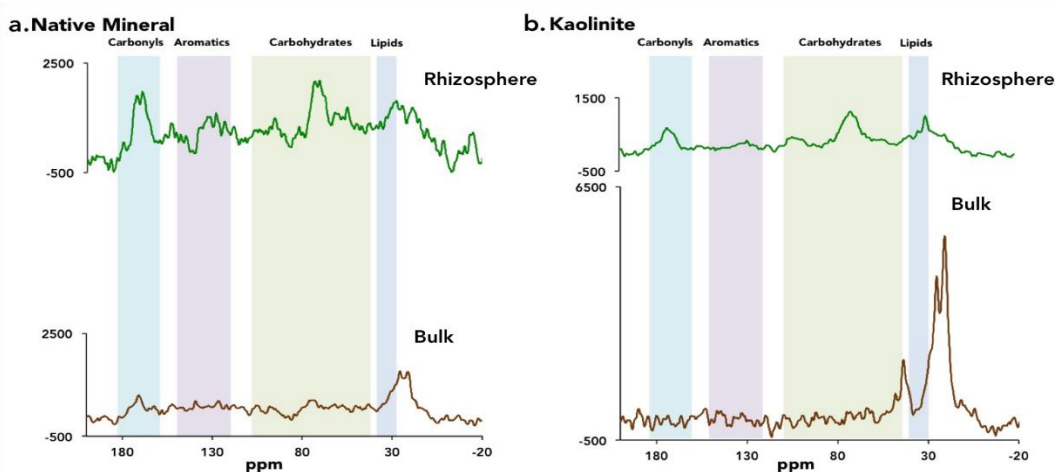


Figure 12. Solid-state ^{13}C -NMR spectra for soil Native Minerals (separated via density fractionation) (a) and Kaolinite minerals (b), incubated for 2 months in annual grassland soil microcosms with rhizosphere and bulk soil treatments. Each spectra represents analysis of 3 pooled biological replicates. Peaks are clustered into broad organic C functional group categories: carboxyls, aromatics, carbohydrates, and lipids.

Conclusion

The LLNL *Microbes Persist* Soil Microbiome SFA uses a multi-domain approach to identify the microbial and viral inhabitants of soil ecosystems, providing a comprehensive understanding of biotic interactions, ecophysiological traits, and the fate of microbiome biomass organic carbon. Our team has led new developments in imaging, mass spectrometry, and related methods that provide direct insight into the biological, chemical and physical processes that contribute to the formation and stabilization of SOM. Going forward, it will be critical to build stronger linkages between methods—including ‘omics approaches—to generate more a comprehensive understanding of samples and systems. We expect the Rhizo-scope and other nondestructive, live imaging methods will bring a better understanding of temporal and spatial phenomena in complex root-microbial-mineral systems. As we add Raman characterization capability and adaptive optics to the Rhizo-scope, this will allow even more detailed molecular characterization of more realistic systems. Ex-situ imaging methods, such as STXM and NanoSIMS, are extremely powerful ways to characterize isotopic-molecular-spatial relationships without artifacts of sample pre-treatment. However, these approaches would benefit from new means of sample preparation that allow correlated imaging of intact samples; cryogenic methods may be particularly useful to hold soils in their native configurations without the addition of fixatives and resins while retaining soluble constituents. These methods would also benefit from increased automation and throughput, including cross-correlation with other imaging methods, such as fluorescence in situ hybridization (FISH) techniques.

In future work, it will be important to better link imaging methods with bulk microbial and SOM characterization methods (e.g metabolomics, transcriptomics) through experiments designed to isolate specific processes. However, soil is a challenging medium for the bulk characterization methods discussed above, due to large number of compounds involved and the potential for important compounds to be rapidly consumed or sorbed by soil components. We see cross-correlation of SOM characterization methods and isotope tracing as key to moving the field forward. By linking the complimentary information gathered via the exquisite mass precision of FTICR-MS, to the ability of NMR (and STXM) to provide general classification of chemical compounds, to inferences gained through SIP-enables metagenome resolved genomics, we envision a more comprehensive understanding of SOM. Moving forward, it will also be important to expand access to databases, instruments, and standards to broaden the base of users and practitioners and promote innovation and integration. Given the complexity of soil, it is only through the integration of imaging and mass spectrometry methods with the full breadth of ‘omics approaches that we will reach a predictive understanding of how soil microbiomes shape the formation and persistence of soil organic matter.

This work, conducted at Lawrence Livermore National Laboratory, was supported by DOE OBER Genomic Sciences award SCW1632 and conducted under the auspices of DOE Contract DE-AC52- 07NA27344.

References

1. Burow*, L.C., D. Woebken*, I.P.G. Marshall, E.A. Lindquist, B.M. Bebout, L. Prufert-Bebout, T.M. Hoehler, S.G. Tringe, J. Pett-Ridge, P.K. Weber, A.M. Spormann and S.W. Singer, *Anoxic carbon flux in photosynthetic microbial mats as revealed by metatranscriptomics*. ISME J, 2013. **7**(4): p. 817-829, *equal contribution
2. Finzi-Hart*, J.A., J. Pett-Ridge*, P.K. Weber, R. Popa, S.J. Fallon, T. Gunderson, I.D. Hutcheon, K.H. Nealson and D.G. Capone, *Fixation and fate of C and N in the cyanobacterium Trichodesmium using nanometer-scale secondary ion mass spectrometry*. Proceedings of the National Academy of Science, USA, 2009. **106**(15): p. 6345-6350 *equal contribution.
3. Popa, R., P.K. Weber, J. Pett-Ridge, J.A. Finzi, S.J. Fallon, I.D. Hutcheon, K.H. Nealson and D.G. Capone, *Carbon and nitrogen fixation and metabolite exchange in and between individual cells of Anabaena oscillarioides*. ISME Journal, 2007. **1**(4): p. 354-360.
4. Woebken, D., L.C. Burow, L. Prufert-Bebout, B.M. Bebout, T.M. Hoehler, J. Pett-Ridge, A.M. Spormann, P.K. Weber and S.W. Singer, *Identification of a novel cyanobacterial group as active diazotrophs in a coastal microbial mat using NanoSIMS analysis*. The ISME Journal, 2012. **6**(7): p. 1427-1439.
5. Pett-Ridge, J. and P.K. Weber, *NanoSIP: NanoSIMS applications for microbial biology*, in *Microbial Systems Biology: Methods and Protocols*, A. Navid, Editor. 2012, Humana Press.
6. Dekas, A.E., R.S. Poretsky and V.J. Orphan, *Deep-Sea Archaea Fix and Share Nitrogen in Methane-Consuming Microbial Consortia*. Science, 2009. **326**(5951): p. 422-426.
7. Pett-Ridge, J. and P.K. Weber, *NanoSIP: NanoSIMS applications for microbial biology*, in *2nd edition of Microbial Systems Biology: Methods and Protocols. Methods in Molecular Biology, Springer Protocols*, A. Navid, Editor. 2021, Humana Press, : New York, <https://doi.org/10.1007/978-1-0716-1585-0>.
8. Hestrin, R., P.K. Weber, J. Pett-Ridge and J. Lehmann, *Plants and mycorrhizal symbionts acquire substantial soil nitrogen from gaseous ammonia transport*. New Phytologist, 2021. <https://doi.org/10.1111/nph.17527>.
9. See, C.R., A.B. Keller, S.E. Hobbie, P.G. Kennedy and J. Pett-Ridge, *Hyphae move matter and microbes to mineral microsites: Integrating the hyphosphere into conceptual models of soil organic matter stabilization*. Global Change Biology (in review).
10. Neurath, R., T. Whitman, I.X. Chu-Jacoby, A.M. Thompson, A. Lipton, M. Tfaily, J. Kyle, K.J. Bloodsworth, D.J. Herman, J. Pett-Ridge and M. Firestone, *Root carbon interaction with soil minerals is dynamic, leaving a legacy of microbially-derived residues*. Environmental Science & Technology, 2021: p. <https://doi.org/10.1021/acs.est.1c00300>.
11. Neurath, R., *Plant-Microbe-Mineral Interactions Control Carbon Persistence in Soil*, in *Environmental Science Policy and Management*. 2020, UC Berkeley.
12. Sommers, P., Chatterjee, A., Varsani, A., Trubl, G. 2021. *Integrating viral metagenomics into an ecological framework* Annual Review of Virology, 2021.
13. Gates, S.D., R.C. Condit, N. Moussatche, B.J. Stewart, A.J. Malkin and P.K. Weber, *High initial sputter rate found for vaccinia virions using isotopic labeling, nanoSIMS, and AFM*. Analytical chemistry, 2018. **90**(3): p. 1613-1620.
14. Pasulka, A.L., K. Thamatrakoln, S.H. Kopf, Y. Guan, B. Poulos, A. Moradian, M.J. Sweredoski, S. Hess, M.B. Sullivan and K.D. Bidle, *Interrogating marine virus-host*

- interactions and elemental transfer with BONCAT and nanoSIMS-based methods.* Environmental microbiology, 2018. **20**(2): p. 671-692.
15. Mayali, X., P.K. Weber, E. Nuccio, J. Lietard, M. Somoza, S.J. Blazewicz and J. Pett-Ridge, *Stable Isotope Probing, Methods and Protocols.* Methods in Molecular Biology, 2019. **2046**: p. 71-87.
 16. Mayali, X., P.K. Weber, E.L. Brodie, S. Mabery, P.D. Hoeplich and J. Pett-Ridge, *High-throughput isotopic analysis of RNA microarrays to quantify microbial resource use.* The ISME Journal, 2012. **6**(6): p. 1210-1221.
 17. Murrell, J.C. and A.S. Whiteley, eds. *Stable Isotope Probing and Related Technologies.* 2011, ASM Press: Washington, D.C. 345.
 18. Mayali, X., P.K. Weber, E.L. Brodie, S. Mabery, P. Hoeplich and J. Pett-Ridge, *High-throughput isotopic analysis of RNA microarrays to quantify microbial resource use* ISME Journal, 2012. **6**: p. 1210-1221.
 19. Mayali, X., P.K. Weber, E. Nuccio, J. Lietard, M. Somoza, S.J. Blazewicz and J. Pett-Ridge, *Chip-SIP: Stable Isotope Probing Analyzed with rRNA-Targeted Microarrays and NanoSIMS,* in *Stable Isotope Probing.* 2019, Springer. p. 71-87.
 20. Mayali, X., P.K. Weber and J. Pett-Ridge, *Taxon-specific C:N relative use efficiency for amino acids in an estuarine community.* FEMS Microbiology Ecology, 2013. **83**(2): p. 402-412.
 21. Nuccio, E.E., N. Nguyen, U. Nunes da Rocha, X. Mayali, J. Bougoure, P.K. Weber, E.L. Brodie, M.K. Firestone and J. Pett-Ridge, *Community RNA-Seq: Multi-kingdom responses to living versus decaying roots in soil.* bioRxiv <https://doi.org/10.1101/2021.01.12.426429>, ISME Communications (in press), 2021.
 22. Pausch, J., S. Kramer, A. Scharroba, N. Scheunemann, O. Butenschoen, E. Kandeler, S. Marhan, M. Riederer, S. Scheu, Y. Kuzyakov and L. Ruess, *Small but active – pool size does not matter for carbon incorporation in below-ground food webs.* Functional Ecology, 2016. **30**(3): p. 479-489.
 23. Keiluweit, M., J.J. Bougoure, L.H. Zeglin, D.D. Myrold, P.K. Weber, J. Pett-Ridge, M. Kleber and P.S. Nico, *Nano-scale investigation of the association of microbial nitrogen residues with iron (hydr)oxides in a forest soil O-horizon.* Geochimica et Cosmochimica Acta, 2012. **95**(0): p. 213-226.
 24. Nicora, C.D., K.E. Burnum-Johnson, E.S. Nakayasu, C.P. Casey, R.A. White III, T.R. Chowdhury, J.E. Kyle, Y.-M. Kim, R.D. Smith and T.O. Metz, *The MPLEx protocol for multi-omic analyses of soil samples.* Journal of visualized experiments: JoVE, 2018(135).
 25. JB, S., L. TY, L.F. 3rd, T. AV, T. N, R. EW, K. DW and P.-T.L. J., *21 Tesla Fourier Transform Ion Cyclotron Resonance Mass Spectrometer Greatly Expands Mass Spectrometry Toolbox.* J Am Soc Mass Spectrom, 2016: p. 1929-1936.
 26. Shaw, J.B., T.-Y. Lin, F.E. Leach III, A.V. Tolmachev, N. Tolić, E.W. Robinson, D.W. Koppenaal and L. Paša-Tolić, *21 Tesla Fourier transform ion cyclotron resonance mass spectrometer greatly expands mass spectrometry toolbox.* Journal of The American Society for Mass Spectrometry, 2016. **27**(12): p. 1929-1936.
 27. Lin, Y., A.N. Campbell, A. Bhattacharyya, N. DiDonato, A.M. Thompson, M.M. Tfaily, P.S. Nico, W.L. Silver and J. Pett-Ridge, *Differential effects of redox conditions on the decomposition of litter and soil organic matter.* Biogeochemistry Letters 2020. **154**: p. 1-15.

28. Masiello, C.A., M.E. Gallagher, J.T. Randerson, R.M. Deco and O.A. Chadwick, *Evaluating two experimental approaches for measuring ecosystem carbon oxidation state and oxidative ratio*. Journal of Geophysical Research: Biogeosciences, 2008. **113**(G3).
29. Pett-Ridge, J., J. Shi, K.Y. Estera-Molina, E.E. Nuccio, M. Yuan, R. Rijkers, T. Swenson, K. Zhalnina, T. Northen, J. Zhou and M.K. Firestone, *Rhizosphere carbon turnover from cradle to grave: the role of microbe-plant interactions*, in *Rhizosphere Biology: Interactions with Plants*, V. Gupta and A.K. Sharma, Editors. 2020, Springer Nature Press.
30. Zhalnina, K., K.B. Louie, Z. Hao, N. Mansoori, U.N. da Rocha, S.J. Shi, H.J. Cho, U. Karaoz, D. Loque, B.P. Bowen, M.K. Firestone, T.R. Northen and E.L. Brodie, *Dynamic root exudate chemistry and microbial substrate preferences drive patterns in rhizosphere microbial community assembly*. Nature Microbiology, 2018. **3**(4): p. 470-480.